JACS
JOURNAL OF THE AMERICAN CHEMICAL SOCIETY
Communication
pubs.acs.org/JACS

Phenylenediamine-Based FeN_x/C Catalyst with High Activity for Oxygen Reduction in Acid Medium and Its Active-Site Probing

Qiang Wang,[†] Zhi-You Zhou,*[,†] Yu-Jiao Lai,[†] Yong You,[‡] Jian-Guo Liu,[‡] Xia-Ling Wu,[†] Ephrem Terefe,[†] Chi Chen,[†,§] Lin Song,[†] Muhammad Rauf,[†] Na Tian,[†] and Shi-Gang Sun*[,†]

[†]State Key Laboratory of Physical Chemistry of Solid Surfaces, Department of Chemistry, College of Chemistry and Chemical Engineering, Xiamen University, Xiamen 361005, China

[‡]Eco-materials and Renewable Energy Research Center, Department of Materials Science and Engineering, and National Laboratory of Solid State Microstructures, Nanjing University, Nanjing 210093, China

[§]State Key Laboratory of Chemical Engineering, East China University of Science and Technology, Shanghai 200237, China

Supporting Information

ABSTRACT: High-temperature pyrolyzed FeN_x/C catalyst is one of the most promising nonprecious metal electrocatalysts for oxygen reduction reaction (ORR). However, it suffers from two challenging problems: insufficient ORR activity and unclear active site structure. Herein, we report a FeN_x/C catalyst derived from poly-*m*-phenylenediamine (P*m*PDA-FeN_x/C) that possesses high ORR activity (11.5 A g^{-1} at 0.80 V vs RHE) and low H_2O_2 yield (<1%) in acid medium. The P*m*PDA-FeN_x/C also exhibits high catalytic activity for both reduction and oxidation of H_2O_2. We further find that the ORR activity of P*m*PDA-FeN_x/C is not sensitive to CO and NO_x but can be suppressed significantly by halide ions (e.g., Cl^-, F^-, and Br^-) and low valence state sulfur-containing species (e.g., SCN^-, SO_2, and H_2S). This result reveals that the active sites of the FeN_x/C catalyst contains Fe element (mainly as Fe^{III} at high potentials) in acid medium.

Proton exchange membrane fuel cell (PEMFC) is a promising clean power source for transportation applications. However, the commercialization of PEMFC is severely hampered by high costs mainly from Pt catalysts, especially for oxygen reduction reaction (ORR).[1] The exploration of nonprecious metal (NPM) catalysts for ORR is an effective approach to reduce the cost.[2] Among NPM catalysts, FeN_x/C catalyst is the most promising candidate because it exhibits considerable ORR activity in acid medium, thus compatible with strong acidic environment of Nafion-based PEMFC that is industrially more mature than alkaline membrane fuel cell.[3] The FeN_x/C catalyst can be prepared through high-temperature pyrolysis of very cheap and abundant precursors, such as the mixture of carbon black, nitrogen-containing species (e.g., polyaniline (PANI), NH_3, and urea) and inorganic iron salts.[4] Recently, great progresses have been made in this field.[3,5] For example, Dodelet's group prepared a FeN_x/C catalyst with high ORR activity even comparable to Pt/C by developing a novel protocol including ball milling of precursors and two-step pyrolysis at different atmosphere.[5a,b] However, the stability of this catalyst is insufficient in acidic medium.[6] In contrast, Zelenay et al. prepared a PANI-based FeN_x/C catalyst with improved durability due to low H_2O_2 yield (<1%) during ORR.[5c] Nevertheless, its ORR activity, ~6.7 A g^{-1} at 0.80 V vs reversible hydrogen electrode (RHE), is not high enough for fuel cell applications.

Besides the catalytic activity and stability, the nature of active sites is a long-debated issue for pyrolyzed FeN_x/C catalyst. The lack of knowledge about active sites has greatly hampered the rational design and preparation of high active and long durable FeN_x/C catalyst. The challenges in active site studies mainly arise from the extremely low density of active sites (e.g., Fe content is <1 wt%) and the complexity of both structure and composition.[3] There is even no consensus whether active sites contain Fe atom or not.[3b,7] Although Fe is needed for high ORR activity, some argued that Fe only promotes the formation of active sites, but it does not directly participate in active site.[7,8] Currently, studies of active sites mainly rely on ex situ spectroscopic methods, such as XPS, Mössbauer spectroscopy, and X-ray absorption spectroscopy (such as EXAFS and XANES),[5f,9] nevertheless, electrochemical methods have not received enough attention. As a matter of fact, electrochemical methods have very high sensitivity and can provide important information for active sites.[10] For example, Gewirth et al. used cyanide (CN^-) as a probe ion and justified that the active site contains iron in alkaline medium for both pristine and pyrolyzed iron phthalocyanine (FePc) catalysts.[10a] However, no corresponding electrochemical tests in acidic medium have been reported so far, mainly due to the formation of highly toxic HCN.

Herein, we report the synthesis of a FeN_x/C catalyst with high ORR activity (11.5 A g^{-1} at 0.80 V) and low H_2O_2 yield (<1%) in acid medium derived from poly-*m*-phenylenediamine (P*m*PDA). The motivation of using P*m*PDA consists in that it contains more nitrogen element (26 vs 15 wt%) and has higher thermostability than PANI.[11] The high thermostability will reduce the nitrogen loss during the heating process. More importantly, we reveal that the active site of the P*m*PDA-FeN_x/C catalyst contains Fe element, and the Fe valence state may be mainly Fe^{III} through systematical investigation of the effects of a series of inorganic molecules (e.g., CO and NO_x) and ions (e.g., Cl^-, F^-, Br^-, SCN^-, SO_3^{2-}, and S^{2-}) on the ORR activity.

Received: June 9, 2014
Published: July 17, 2014

dx.doi.org/10.1021/ja505777v | J. Am. Chem. Soc. 2014, 136, 10882−10885

The P*m*PDA-FeN$_x$/C catalyst was synthesized through high-temperature pyrolysis of the precursor containing P*m*PDA-coated carbon black and $FeCl_3$ (see Figure S1). In brief, prior to polymer coating, carbon black (Ketjenblack EC600JD) surface was modified with hydrophilic sulfophenyl (-Ph-SO_3H) group to improve the dispersion of carbon black in aqueous solution and the affinity to P*m*PDA. After the surface modification, the average diameter of carbon agglomerates in solution has decreased from 49 to 5.2 μm (Figure S2). The surface-modified carbon black was coated with P*m*PDA through oxidative polymerization of *m*-PDA monomer by $(NH_4)_2S_2O_8$. The P*m*PDA-coated carbon black was cleaned and mixed with $FeCl_3$, and then subjected to first pyrolysis, acid-washing, and second pyrolysis protocol (Figures S1 and S3) according to the literature methods.[5c,g] The pyrolysis temperature varied from 600 to 1000 °C. The best catalyst prepared at 950 °C has microporous structure with a BET surface area of about 650 $m^2\ g^{-1}$ (Figure S4).

Figure 1a shows the ORR polarization curves and H_2O_2 yield plots on the P*m*PDA-FeN$_x$/C catalyst prepared at different pyrolysis temperature, measured on a rotating ring-disc electrode (RRDE) in O_2-saturated 0.1 M H_2SO_4 solution. The background capacitive current has been corrected (Figure S5). At pyrolysis temperature of 600 °C, the catalyst has very low ORR activity and high H_2O_2 yield (13% at 0.70 V). Along with increasing pyrolysis temperature, the ORR activity increases quickly, reaches a maximum at 950 °C, and then declines at 1000 °C. H_2O_2 yield shows opposite trend with a minimal value of 0.80% (at 0.70 V) at 950 °C. The kinetic mass activity (j_m) at 0.80 V, which is usually used to evaluate the activity of FeN$_x$/C in the RRDE test, was calculated through Koutecky–Levich equation for mass transfer correction and then was normalized by the catalyst loading (0.6 mg cm^{-2}). Figure 1b depicts the dependence of mass activity on the pyrolysis temperature. As for the best sample obtained at 950 °C, the half-wave potential ($E_{1/2}$) is about 0.82 V, just 65 mV gap compared with commercial Pt/C (Figure S6).

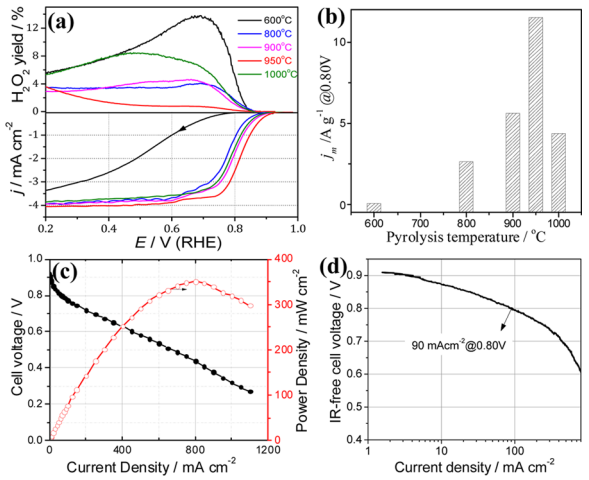

Figure 1. (a) ORR polarization curves and H_2O_2 yield plots of P*m*PDA-FeN$_x$/C catalyst prepared at different pyrolysis temperature, measured in O_2-saturated 0.1 M H_2SO_4. Catalyst loading: 0.6 mg cm^{-2}; Scan rate: 10 mV s^{-1}; Rotating speed: 900 rpm. (b) Variety of ORR mass activity at 0.80 V with pyrolysis temperature. (c) Polarization and power density plots for H_2O_2 single fuel cell with P*m*PDA-FeN$_x$/C as cathode catalyst at 80 °C. MEA active area: 2.0 cm^2; Nafion 211 membrane; Cathode catalyst loading: 4 mg cm^{-2}; Anode catalyst: Pt/C (60 wt%, JM) with Pt loading of 0.5 mg cm^{-2}. No back pressure was applied. (d) Plot of *iR*-free cell voltage versus the logarithm of current density.

The j_m at 0.80 V is 11.5 A g^{-1}, that is larger than the values of pyrolyzed Hemin (3.6 A g^{-1}),[12] PANI-based FeN$_x$/C catalyst (~6.7 A g^{-1}),[5c] carbon nanotube–graphene complexes (4.4–10.5 A g^{-1}),[5f,13] and VB12-based mesoporous FeN$_x$/C (5.0 A g^{-1}),[14] though is inferior to transition-metal-doped ordered mesoporous porphyrinic carbons (45 A g^{-1}, yet relatively high H_2O_2 yield of 6%).[15] The reproducibility of preparing P*m*PDA-FeN$_x$/C is fairly good, with the j_m at 0.80 V varying from 10 to 14 A g^{-1} and H_2O_2 yield varying from 0.5% to 1.5% for over 20-batch syntheses. If P*m*PDA-FeN$_x$/C catalyst was prepared from pristine carbon black, the activity is significantly low, only about 5.2 A g^{-1} (Figure S6).

We further carried out preliminary fuel cell test by employing the P*m*PDA-FeN$_x$/C (950 °C) as cathode catalyst. Figure 1c shows the fuel cell polarization curve and power density plot. The maximal power density can reach to 350 mW cm^{-2} at cell voltage of 0.44 V and current density of 800 mA cm^{-2}. Figure 1d illustrates *iR*-free polarization plot versus the logarithm of current density. The current density at 0.80 V is about 90 mA cm^{-2}. Note that no back pressure was applied during the fuel cell test here, so the partial pressures of O_2 and H_2 were about 0.53 bar on accounting the saturation water vapor pressure of 0.47 bar at 80 °C. On basis of kinetic equation and the reaction order of O_2 (~0.79) and H_2 (~0.50) in PEMFC,[16] the activity of P*m*PDA-FeN$_x$/C under reference condition of 1 bar of O_2 and H_2 was estimated to be 205 mA cm^{-2}, or 51 A g^{-1}.

ORR can occur through two typical pathways, that is, direct 4e pathway ($O_2 + 4H^+ + 4e = 2H_2O$, E° = 1.229 V) and indirect pathway via H_2O_2 intermediate ($O_2 + 2H^+ + 2e = H_2O_2$ E° = 0.695 V; $H_2O_2 + 2H^+ + 2e = 2H_2O$, E° = 1.763 V). The contribution of two pathways can be revealed by determining the H_2O_2 yield and its dependence on catalyst loading.[17] The P*m*PDA-FeN$_x$/C catalyst has a low H_2O_2 yield (<1% when E > 0.45 V) under high catalyst loading of 0.6 mg cm^{-2} (Figure 1a), suggesting that the ORR passes mainly via direct 4e pathway. However, we found that the H_2O_2 yield increases significantly with decreasing catalyst loading, as shown in Figures 2a and S7. For example, it reached up to 16% when catalyst loading decreased to 0.06 mg cm^{-2}. We further found that the P*m*PDA-FeN$_x$/C has high catalytic activity toward both electrochemical reduction and oxidation of H_2O_2. As illustrated in Figure 2b, the

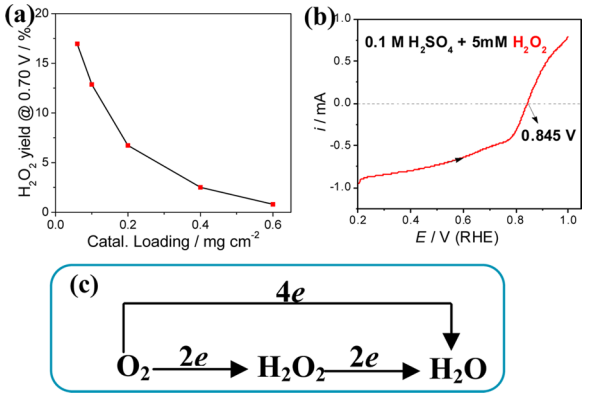

Figure 2. (a) Dependence of H_2O_2 yield at 0.70 V on the P*m*PDA-FeN$_x$/C (950 °C) catalyst loading on the electrode surface. (b) Polarization curve of H_2O_2 reduction and oxidation on P*m*PDA-FeN$_x$/C (950 °C) catalyst in 0.1 M H_2SO_4 + 5 mM H_2O_2. Catalyst loading: 0.6 mg cm^{-2}; rotating speed: 900 rpm. (c) Illustration of both direct 4e and indirect 2e + 2e pathways involved in ORR on P*m*PDA-FeN$_x$/C.

dx.doi.org/10.1021/ja505777v | J. Am. Chem. Soc. 2014, 136, 10882–10885

polarization curve of H_2O_2 reduction and oxidation is continuous with a zero-crossing potential of 0.845 V, about 0.09 V lower than that of Pt.[18] At 0.80 V, the H_2O_2 reduction current is close to the diffusion-limited current. It is known that the performance of FeN_x/C catalysts greatly depends on preparation conditions. The cases of very poor catalytic activity for H_2O_2 reduction,[17a] and extremely high H_2O_2 yield (80−100%) for ORR,[17b] have been reported. On basis of our experimental results of high loading-dependent H_2O_2 yield and high H_2O_2 reduction activity (Figure 2a,2b), it is reasonable to claim that the indirect pathway is involved for ORR on P*m*PDA-FeN_x/C catalyst. On the other hand, considering the much higher onset potential of ORR (~0.94 V) than standard electrode potential for O_2 reduction to H_2O_2 (E° = 0.695 V), as well as very low H_2O_2 yield at E > 0.80 V (Figure 1a), the direct 4e pathway should also be included, especially at high electrode potential.

As for active site studies, although XPS analysis demonstrates that the P*m*PDA-FeN_x/C catalyst contains C, N, and Fe elements and the N 1s spectra can be further deconvolved into five N species (i.e., cyano-, pyridinic-, pyrrolic-, graphitic-N and Fe-N) based on the literature methods,[9c] none of them can well correlate with the ORR activity (Figure S8). Alternatively, electrochemical studies of the susceptibility and reactivity of the FeN_x/C catalyst to other molecules besides O_2 may also provide valuable information for understanding active site nature. It is known that, in biological systems, CO and NO are two poisoning species to hemoglobin and myoglobin by binding to Fe porphyrin. However, we found that CO and NO_x can not influence the ORR activity of the P*m*PDA-FeN_x/C catalyst. Figure 3a illustrates the ORR polarization curves of pure O_2 and

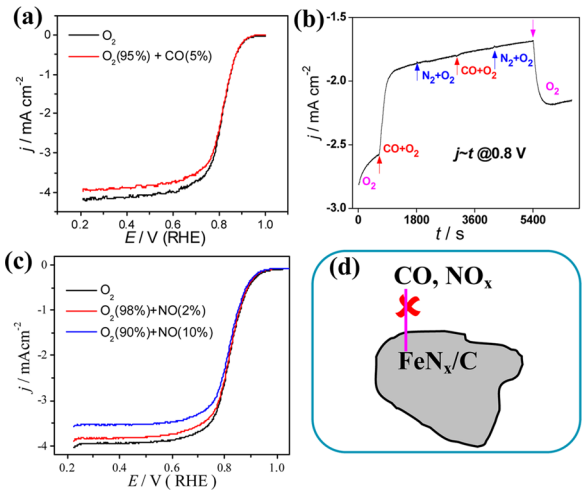

Figure 3. Effect of CO and NO_x on the ORR activity of P*m*PDA-FeN_x/C (950 °C) catalyst in 0.1 M H_2SO_4. (a) ORR polarization curves with pure O_2 and O_2 (95%) + CO (5%) mixture gas. (b) Current−time curve recorded at 0.80 V with reactant gas switching among pure O_2, O_2 (80%) + CO (20%) and O_2 (80%) + N_2 (20%) mixture gas. (c) ORR polarization curves with pure O_2 and mixture gas containing 2% or 10% NO. (d) Illustration of negligible effect of CO and NO_x on the ORR of FeN_x/C catalysts.

O_2 (95%) + CO (5%) mixture gas. No discernible difference can be observed in the kinetic-control region (0.8−0.90 V), and the slight decrease in diffusion-limited current is due to the low O_2 partial pressure (P_{O_2}) in the mixture gas. Previously, Dodelet's group observed that ORR activity of pyrolyzed Fe porphyrins can be restored after switching gas from pure CO to O_2.[10b] However, their experiment was carried out in diffusion-limited region, where ORR current is insensitive to intrinsic catalytic activity. Furthermore, large current fluctuation induced by the change of P_{O_2} may overwhelm the possible slight change of ORR activity by CO. To avoid these questions, we carried out a test under a fixed P_{O_2} (Figure 3b). In the O_2 presaturation 0.1 M H_2SO_4 solution, the potential was held at 0.80 V (kinetic region) for 650 s, then the bubbling gas was switched from pure O_2 to O_2 (80%) + CO (20%) mixture gas. The ORR current decreases quickly from 2.57 to 1.95 mA cm^{-2} due to the decrease of P_{O_2}. At about 1800 s, the gas was changed into O_2 (80%) + N_2 (20%) with the same P_{O_2}, and the switch procedure was repeated and finally back to pure O_2 at 5400 s. Clearly, there is no change of ORR current when the bubbling gas was switched between O_2 + CO and O_2 + N_2. As for NO, we tested two NO content (2% and 10%) in the O_2 + NO mixture gas (partial NO has been oxidized by O_2 to brown NO_2). As illustrated in Figure 3c, the effect of NO_x in the kinetic region is also negligible. These results indicate that both CO and NO_x can not bind to the active site of FeN_x/C catalyst (Figure 3d). It has been reported that CO can bind to Fe^{II} porphyrins but can not to Fe^{III} porphyrins.[19] The insensitivity of P*m*PDA-FeN_x/C to CO and NO_x suggests that Fe valence state may be Fe^{III} if active site contains iron atom.

Although the P*m*PDA-FeN_x/C is not sensitive to CO and NO_x, we found that halide and pseudohalide ions can suppress the ORR activity. Figure 4 compares the polarization curves of P*m*PDA-FeN_x/C in the 0.1 M H_2SO_4 solution before and after adding 5 mM of F^-, Cl^-, Br^-, and SCN^- ions. It is known that SCN^- ion can be oxidized at E > 0.77 V in the forward scan, but the forward and backward ORR polarization curves are nearly overlapped after N_2-background subtracting (Figure S9). The negative shift of the $E_{1/2}$ follows the order of SCN^- > Cl^- > F^- >

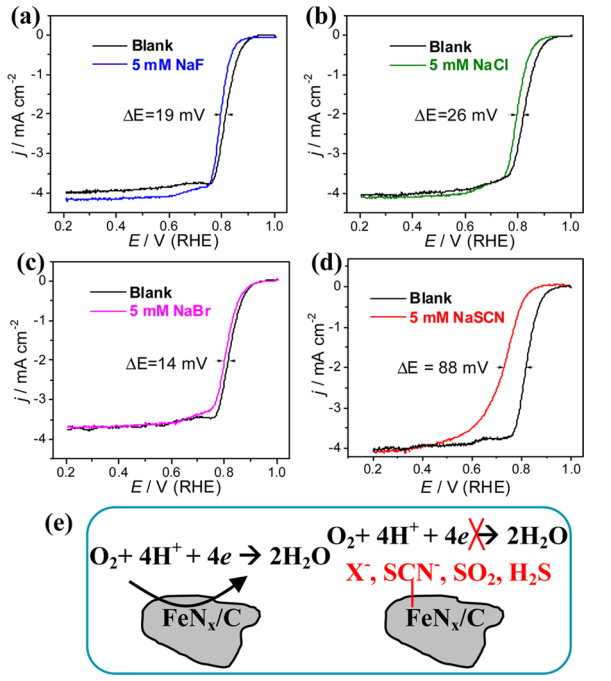

Figure 4. Effects of (a) F^-, (b) Cl^-, (c) Br^-, and (d) SCN^- ions on ORR activity of P*m*PDA-FeN_x/C (950 °C) catalyst in 0.1 M H_2SO_4. All above four ion concentrations were 5 mM; Catalyst loading: 0.6 mg cm^{-2}; Rotating speed: 900 rpm. (d) Illustration of halide ions and S-containing species on the ORR of FeN_x/C catalyst.

dx.doi.org/10.1021/ja505777v | J. Am. Chem. Soc. 2014, 136, 10882−10885

Br^-, being 88, 26, 19, and 14 mV, respectively. The kinetic current density at 0.80 V has been decreased by 18 times for 5 mM SCN^-. This result clearly indicates that the active site of P*m*PDA-FeN_x/C should contain Fe element because these anions have high affinity to Fe ion. Since F^- and Fe^{3+} can form very stable $[FeF_6]^{3-}$ complex, but F^- and Fe^{2+} cannot, the considerable strong effect of F^- ion further suggests that the dominant valence state of Fe element in active site is Fe^{III} during ORR, especially at high potential ($E > 0.7$ V). Furthermore, we explored the effect of chalcogen compounds and found that 1 mM of SO_3^{2-} or S^{2-} (real forms are SO_2 and H_2S in acid solution, respectively) can also seriously inhibit the ORR activity (the potential are negatively shift by 40 and 70 mV, respectively), but SeO_2 and TeO_3^{2-} have no influence (Figures S10−S11). The above results demonstrate that low valence state sulfur-containing species are generally poisonous for the P*m*PDA-FeN_x/C catalyst. However, such degradation effect is much less than that for Pt catalyst. For example, 0.1 mM of SCN^- or H_2S can completely suppress the ORR activity of Pt electrode (Figure S12). As for the effect of SCN^- concentration on P*m*PDA-FeN_x/C catalyst, we have observed that the ORR activity greatly decreased by the initial 1 mM SCN^- and gradually approached stable value when SCN^- increases to 5 mM (Figure S13).

In conclusion, we have prepared a FeN_x/C catalyst with high ORR activity and low H_2O_2 yield in acidic solution by employing nitrogen-rich P*m*PDA as precursor. The P*m*PDA-FeN_x/C exhibits also high catalytic activity for both reduction and oxidation of H_2O_2. Through systematic investigations of the effects of a series of inorganic molecules and ions on the ORR activity, we found that halide ions (e.g., Cl^-, F^-, and Br^-) can slightly suppress, while low valence state sulfur-containing species (e.g., SCN^-, SO_2, and H_2S) can significantly suppress the ORR activity. These results suggest that the active site of the FeN_x/C in acidic solutions contains Fe element, and its valence state is mainly Fe^{III} since this catalyst is not sensitive to CO and NO_x but distinctly sensitive to F^- ion. The present study has thrown a new insight into the active site nature of the FeN_x/C through molecule/ion probes and is of importance in rational design of high performance FeN_x/C catalysts for the ORR.

■ ASSOCIATED CONTENT

Supporting Information

Catalyst synthesis details; TEM, XPS, and supplement electrochemical tests. This material is available free of charge via the Internet at http://pubs.acs.org.

■ AUTHOR INFORMATION

Corresponding Authors

zhouzy@xmu.edu.cn
sgsun@xmu.edu.cn

Notes

The authors declare no competing financial interest.

■ ACKNOWLEDGMENTS

This work was supported by grants from Major State Basic Research Development Program of China (2012CB215500), Natural Science Foundation of China (21373175, 21361140374, and 21321062), Fundamental Research Funds for the Central Universities (2012121019), Program for New Century Excellent Talents in University (NECT-11-0301), and NFFTBS (J1310024). We thank Yan-Ping Zheng in Xiamen University for XPS test.

■ REFERENCES

(1) Borup, R.; et al. *Chem. Rev.* **2007**, *107*, 3904−3951.
(2) Su, D. S.; Sun, G. Q. *Angew. Chem., Int. Ed.* **2011**, *50*, 11570−11572.
(3) (a) Chen, Z.; Higgins, D.; Yu, A.; Zhang, L.; Zhang, J. *Energy Environ. Sci.* **2011**, *4*, 3167−3192. (b) Jaouen, F.; Proietti, E.; Lefevre, M.; Chenitz, R.; Dodelet, J. P.; Wu, G.; Chung, H. T.; Johnston, C. M.; Zelenay, P. *Energy Environ. Sci.* **2011**, *4*, 114−130.
(4) Gupta, S.; Tryk, D.; Bae, I.; Aldred, W.; Yeager, E. *J. Appl. Electrochem.* **1989**, *19*, 19−27.
(5) (a) Proietti, E.; Jaouen, F.; Lefevre, M.; Larouche, N.; Tian, J.; Herranz, J.; Dodelet, J. P. *Nat. Commun.* **2011**, *2*, 416. (b) Lefevre, M.; Proietti, E.; Jaouen, F.; Dodelet, J. P. *Science* **2009**, *324*, 71−74. (c) Wu, G.; More, K. L.; Johnston, C. M.; Zelenay, P. *Science* **2011**, *332*, 443−447. (d) Choi, J. Y.; Hsu, R. S.; Chen, Z. W. *J. Phys. Chem. C* **2010**, *114*, 8048−8053. (e) Ding, W.; Wei, Z. D.; Chen, S. G.; Qi, X. Q.; Yang, T.; Hu, J. S.; Wang, D.; Wan, L. J.; Alvi, S. F.; Li, L. *Angew. Chem., Int. Ed.* **2013**, *52*, 11755−11759. (f) Zhang, S. M.; Liu, B.; Chen, S. L. *Phys. Chem. Chem. Phys.* **2013**, *15*, 18482−18490. (g) Liu, G.; Li, X. G.; Ganesan, P.; Popov, B. N. *Appl. Catal., B* **2009**, *93*, 156−165. (h) Liu, J.; Sun, X. J.; Song, P.; Zhang, Y. W.; Xing, W.; Xu, W. L. *Adv. Mater.* **2013**, *25*, 6879−6883.
(6) Herranz, J.; Jaouen, F.; Lefevre, M.; Kramm, U. I.; Proietti, E.; Dodelet, J. P.; Bogdanoff, P.; Fiechter, S.; Abs-Wurmbach, I.; Bertrand, P.; Arruda, T. M.; Mukerjee, S. *J. Phys. Chem. C* **2011**, *115*, 16087−16097.
(7) Matter, P. H.; Wang, E.; Arias, M.; Biddinger, E. J.; Ozkan, U. S. *J. Phys. Chem. B* **2006**, *110*, 18374−18384.
(8) (a) Nallathambi, V.; Lee, J. W.; Kumaraguru, S. P.; Wu, G.; Popov, B. N. *J. Power Sources* **2008**, *183*, 34−42. (b) Woods, M. P.; Biddinger, E. J.; Matter, P. H.; Mirkelamoglu, B.; Ozkan, U. S. *Catal. Lett.* **2010**, *136*, 1−8.
(9) (a) Lefevre, M.; Dodelet, J. P.; Bertrand, P. *J. Phys. Chem. B* **2002**, *106*, 8705−8713. (b) Ramaswamy, N.; Tylus, U.; Jia, Q.; Mukerjee, S. *J. Am. Chem. Soc.* **2013**, *135*, 15443−15449. (c) Artyushkova, K.; Kiefer, B.; Halevi, B.; Knop-Gericke, A.; Schlogl, R.; Atanassov, P. *Chem. Commun.* **2013**, *49*, 2539−2541.
(10) (a) Thorum, M. S.; Hankett, J. M.; Gewirth, A. A. J. *Phys. Chem. Letters* **2011**, *2*, 295−298. (b) Birry, L.; Zagal, J. H.; Dodelet, J. P. *Electrochem. Commun.* **2010**, *12*, 628−631.
(11) Chan, H. S. O.; Ng, S. C.; Hor, T. S. A.; Sun, J.; Tan, K. L.; Tan, B. T. G. *Eur. Polym. J.* **1991**, *27*, 1303−1308.
(12) Wang, Q.; Zhou, Z.; Chen, D.; Lin, J.; Ke, F.; Xu, G.; Sun, S. *Sci. China-Chem.* **2010**, *53*, 2057−2062.
(13) Li, Y.; Zhou, W.; Wang, H.; Xie, L.; Liang, Y.; Wei, F.; Idrobo, J. C.; Pennycook, S. J.; Dai, H. *Nat. Nanotechnol.* **2012**, *7*, 394−400.
(14) Liang, H. W.; Wei, W.; Wu, Z. S.; Feng, X. l.; Müllen, K. *J. Am. Chem. Soc.* **2013**, *135*, 16002−16005.
(15) Cheon, J. Y.; Kim, T.; Choi, Y.; Jeong, H. Y.; Kim, M. G.; Sa, Y. J.; Kim, J.; Lee, Z.; Yang, T. H.; Kwon, K.; Terasaki, O.; Park, G. G.; Adzic, R. R.; Joo, S. H. *Sci. Rep.* **2013**, *3*, 2045−2322.
(16) Jaouen, F.; Herranz, J.; Lefevre, M.; Dodelet, J. P.; Kramm, U. I.; Herrmann, I.; Bogdanoff, P.; Maruyama, J.; Nagaoka, T.; Garsuch, A.; Dahn, J. R.; Olson, T.; Pylypenko, S.; Atanassov, P.; Ustinov, E. A. *ACS Appl. Mater. Interfaces* **2009**, *1*, 1623−1639.
(17) (a) Jaouen, F.; Dodelet, J. P. *J. Phys. Chem. C* **2009**, *113*, 15422−15432. (b) Bonakdarpour, A.; Lefevre, M.; Yang, R.; Jaouen, F.; Dahn, T.; Dodelet, J. P.; Dahn, J. R. *Electrochem. Solid-State Lett.* **2008**, *11*, B105−B108.
(18) Katsounaros, I.; Schneider, W. B.; Meier, J. C.; Benedikt, U.; Biedermann, P. U.; Auer, A. A.; Mayrhofer, K. J. J. *Phys. Chem. Chem. Phys.* **2012**, *14*, 7384−7391.
(19) Ma, M.; Yan, Y. G.; Huo, S. J.; Xu, Q. J.; Cai, W. B. *J. Phys. Chem. B* **2006**, *110*, 14911−14915.